A Modified Meshless Local Petrov-Galerkin Applied to Electromagnetic Axisymmetric Problems

Ramon D. Soares[1], Fernando J. S. Moreira[2], Renato C. Mesquita[3], David A. Lowther[4], Naísses Z. Lima[1]
[1]Graduate Program in Electrical Engineering, Federal University of Minas Gerais, Brazil
[2]Department of Electronic Engineering, [3]Department of Electrical Engineering, Federal University of Minas Gerais, Brazil
[4]Department of Electrical and Computer Engineering, McGill University, Canada
ramon_dornelas@yahoo.com.br, renato@ufmg.br, fernandomoreira@ufmg.br,
david.lowther@mcgill.ca, naisseszoia@gmail.com

***Abstract*—A modified Meshless Local Petrov-Galerkin for an electromagnetic axisymmetric problem is presented in this paper. The method uses the shape functions generated by the Radial Point Interpolation Method with a modified T-scheme to select the support nodes, and also a new and malleable strategy to determine the test domains. The convergence of the method is evaluated using a coaxial cavity problem and it is compared to the Finite Element Method for two different meshes, a good quality one and other composed partially by bad quality elements.**

***Index Terms*—Convergence of Numerical Methods, Integral Equations, Finite Element Method.**

I. Introduction

Several meshless methods are reported in the literature, among them are the Element-Free Galerkin (EFG) [1], the Meshless Local Petrov-Galerkin (MLPG) [2], and the Point Interpolation Methods (PIM) [3]. Meshless methods use a procedure to build their shape functions such as the Moving Least Squares (MLS) and the Point Interpolation Method [4].

In this work, the formulation is based on the MLPG method, which has a local weak formulation, resulting in sparse matrices and minimization of the numerical effort. The Radial Point Interpolation Method with Polynomials (RPIMp) is used to generate the shape functions. In RPIMp, radial basis functions and polynomials are added to the base, providing high accuracy and ensuring consistency of the shape functions [4]. RPIMp shape functions have the Kronecker delta property and thus essential boundary conditions are naturally enforced.

The MLPG does not require any mesh or grid, however a special data structure (generally a k-d tree) is used to determine the support and test domains [4]. In order to improve the MLPG performance, in this paper we use a mesh to do this. A modified T6-scheme is used to select the support nodes to generate the shape function [4]. Using mesh information to determine the test domain, the local weak form integration procedure is simplified and more precision can be obtained, specially in complex geometries. We obtain a MLPG method that depends on a mesh. The advantage of using it is that this mesh can be of bad quality, because it does not affect the obtained results in the same way as it does with the Finite Element Method (FEM). To show this, a coaxial cavity has its modes computed by both methods, using two meshes: a good quality one and another composed partially of bad quality elements. The results show that the proposed MLPG method is much less sensitive to the bad mesh quality than FEM.

II. The Modified MLPG

We will solve an electromagnetic problem with axial symmetry, with the magnetic field having only the H_ϕ component and $\partial H_\phi/\partial\phi = 0$ (which is a 2 dimension analysis, on the $\rho - z$ semi-plane). The global weak-form for the problem is [5]:

$$\oint_{\partial\Omega} \frac{\psi}{\rho\epsilon_r}\frac{\partial(\rho H_\phi)}{\partial n}dl - \iint_\Omega \frac{1}{\rho\epsilon_r}\nabla\psi\cdot\nabla(\rho H_\phi)dA + k_0^2\iint_\Omega \frac{\mu_r\psi}{\rho}(\rho H_\phi)dA = 0. \quad (1)$$

where ϵ_r and μ_r are relative permittivity and permeability, respectively. $\psi(\rho, z)$ is the test function, Ω is the problem domain, and k_0 is the free-space wavenumber.

The MLPG uses a set of nodes inside Ω (interior nodes) and at its boundary $\partial\Omega$ (boundary nodes). The MLPG solution of (1) is achieved by approximating ρH_ϕ by a RPIMp representation [4]. The RPIMp shape function is built using a modified T6-scheme to select the nodes of the support domain: 6 nodes are selected for an interior cell, as suggested by the T6-scheme (3 vertices plus 3 remote vertices of the three neighboring cells), and only 5 nodes are selected for a boundary cell (3 vertices plus 2 remote vertices of neighboring cells). This proposed T-Scheme doesn't use a search structure for adding a node to the boundary cells, which is simpler, efficient, and also provides good results.

For a given node i, its test function ψ_i has a compact support where $\psi_i \neq 0$, which defines the node's test domain Ω_{S_i}, where weak-form integrations are evaluated. We propose to use the mesh to determine Ω_{S_i}, which is composed by all the cells that have a node i as one of its vertices.The adopted test function has a unit value inside Ω_{S_i} and on $\partial\Omega_{S_i}$.

The MLPG local weak form is then obtained from (1) by replacing ψ by 1 and ρH_ϕ by its RPIMp approximation. In (1) the second integral vanishes, as $\nabla\psi = 0$ inside the test domain Ω_{S_i}. The boundary integral of (1) is evaluated only for the $\partial\Omega_{S_i}$ inside Ω_S. For the $\partial\Omega_{S_i}$ on $\partial\Omega$ (assumed to be a perfect electric conductor wall), the boundary integral is used to impose the Neumann boundary condition $\partial(\rho H_\phi)/\partial n = 0$.

III. Numerical Results and Conclusions

Numerical results are presented for the resonant modes of an axially symmetric coaxial cavity which has analytical solution [6]. The analyzed cavity has an internal radius of 1m, an external radius of 2m, a height equal to 1m, and vacuum in its interior ($\epsilon_r = 1$ and $\mu_r = 1$).

MLPG convergence is determined and compared to FEM. Two different meshes are used: the first one (mesh A) has only high quality elements and the second one (mesh B) is partially built with bad quality elements with one internal angle close to 180°. Fig. 1 presents the convergence for the second mode k_2 of the coaxial cavity. The MLPG convergence results are better than the FEM results for both meshes. The MLPG rates are 2.1179 and 1.441 and the FEM ones are 1.9327 and 1.2595 for meshes A and B, respectively. Fig. 1 also presents the parameter δ_j that defines the logarithmic level difference between FEM and MLPG errors at each point j of the curves. The average logarithmic level difference δ_{av} is computed using all δ_j with the same number of nodes. In Fig. 1, $\delta_{av} = 0.5066$ and $\delta_{av} = 1.1682$ for mesh A and B, respectively. These two positive values show that MLPG error curves are below the FEM curves for both meshes. It also can be observed that δ_{av} is increased from mesh A to mesh B, which indicates the lower sensitivity of MLPG to the mesh distortion.

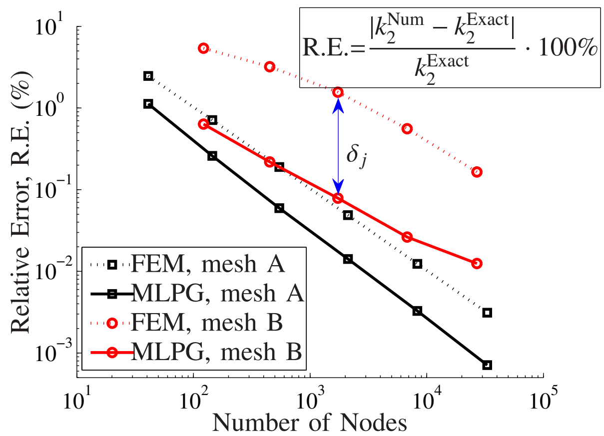

Figure 1: FEM and MLPG convergence using meshes A and B for the second mode of the coaxial cavity. k_2^{Num} and k_2^{Exact} are the numerical and exactly solutions of the second mode.

The convergence rates of the first five modes are shown in Table I, which presents the results for the FEM using meshes A and B (FEM-A and FEM-B), and for the MLPG using the same meshes (MLPG-A and MLPG-B). For the regular mesh A, MLPG has higher convergence rates than FEM for modes k_2 and k_5, and FEM has better results for the other modes. The convergence rates are quite similar, showing that FEM and MLPG have similar performance for the regular mesh. However, regarding the bad quality mesh B, MLPG has higher convergence rates than FEM for four modes while FEM has a slightly larger rate only for mode k_4, showing that MLPG achieves a better performance than FEM for this mesh.

Table I: MLPG and FEM convergence rates.

Modes	k_1	k_2	k_3	k_4	k_5
FEM-A	2.0928	1.9327	1.9809	2.0924	1.9347
MLPG-A	1.965	2.1179	1.9629	1.9804	2.0517
FEM-B	2.1059	1.2595	1.7622	2.0835	1.4020
MLPG-B	2.1558	1.4410	1.8452	2.0494	1.6334

The average logarithmic level difference for MLPG and FEM error curves are shown in Table II for the first five modes of the cavity. δ_{av} are presented for the two meshes A and B (δ_{av}-A and δ_{av}-B). For mesh A, the MLPG has better results for the modes k_2 and k_5, which are below the FEM error curves by 0.5066 and 0.4959 on average. FEM has better results for the modes k_1, k_3, and k_4, which are below the MLPG curves by 0.1885, 0.0134, and 0.2645 on the average. For mesh B, MLPG does not provide a better result only for mode k_4. δ_{av} has little change for mode k_4 and has significant changes for the other modes (δ_{av} of k_5 increases close to 3 times). These average logarithmic level difference results also show the better performance of the proposed MLPG for the worst quality mesh (mesh B).

Table II: Average logarithmic level difference.

Modes	k_1	k_2	k_3	k_4	k_5
δ_{av}-A	-0.1885	0.5066	-0.0134	-0.2645	0.4959
δ_{av}-B	0.3404	1.1682	0.2861	-0.2877	1.4833

These results suggest a better performance of the proposed MLPG than FEM in problems with meshes with bad shaped elements. This is a result that drives our work on the extension of the method for 3 dimension problems where, depending on the geometry, good quality meshes are very difficult to obtain.

Acknowledgment

This work was partially supported by "Numerical Investigation of Coupled Electromagnetic Field Problems", UFMG (Brazil) and McGill University (Canada), CAPES-DFAIT, by CNPQ and by FAPEMIG.

References

[1] E. H. R. Coppoli, R. C. Mesquita, and R. S. Silva, "Induction Machines Modeling With Meshless Methods", *IEEE Trans. Magnetics*, vol. 48, no. 2, pp. 847-850, 2012.

[2] W. Nicomendes, R. Mesquita, and F. Moreira, "Calculating the Band Structure of Photonic Crystals Through the Meshless Local Petrov-Galerkin (MLPG) Method and Periodic Shape Functions", *IEEE Trans. Magnetics*, vol. 48, no. 2, pp. 551-554, 2012.

[3] N. Z. Lima, A. R. Fonseca, and R. C. Mesquita, "Application of Local Point Interpolation Method to Electromagnetic Problems With Material Discontinuities Using a New Visibility Criterion",*IEEE Trans. Magnetics*, vol. 48, no. 2, pp. 615-618, 2012.

[4] G. Liu, *Mesh Free Methods: Moving Beyond the Finite Element Method*, 2nd Ed., CRC Press, 2009.

[5] A. Peterson, S. Ray, and R. Mittra, *Computational Methods for Electromagnetics*, IEEE Press, 1998, pp. 3-332.

[6] R. F. Harrington, *Time Harmonic Eletromagnetic Field*, John Wiley & Sons, 2001, pp. 198-256.